Mercado, E. J. M., Yuan, C., Zhou, Y., Li, J., Edgar, J. H., & Kuball, M. H. H. (2020). Isotopically Enhanced Thermal Conductivity in Few-Layer Hexagonal Boron Nitride: Implications for Thermal Management. *ACS Applied Nano Materials*, *3*(12). https://doi.org/10.1021/acsanm.0c02647

Isotopically Enhanced Thermal Conductivity in Few-layer Hexagonal Boron Nitride: Implications for Thermal Management

Elisha Mercado[1,‡,], Chao Yuan[1,‡], Yan Zhou[1], Jiahan Li[2], James H. Edgar[2], Martin Kuball[1,*]*

1 Center for Device Thermography and Reliability (CDTR), H. H. Wills Physics Laboratory, University of Bristol, BS8 1TL Bristol, UK.

2 Tim Taylor Department of Chemical Engineering, Kansas State University, Manhattan, KS 66506, USA

‡These authors contributed equally to this work

* Corresponding authors: elisha.mercado@bristol.ac.uk; martin.kuball@bristol.ac.uk

Abstract

Hexagonal boron nitride (h-BN) has been highlighted as a promising low-dimensional material for thermal management of next-generation devices. Theory predicts that the thermal conductivity of h-BN increases above the bulk value as the thickness is reduced, but previous reports on few-layer (5-11 layer) h-BN have shown the opposite trend. We investigated the effect of isotopic engineering on the thermal properties of 11-layer h-BN single-crystal flakes. The thermal conductivities of natural (22% ^{10}B, 78% ^{11}B) and monoisotopic (99% ^{10}B) h-BN were determined by a modified optothermal Raman method in the range 300-400K. At room temperature, values were as high as (630 +90/-65) $Wm^{-1}K^{-1}$ for monoisotopic h-^{10}BN and (405 +87/-65) $Wm^{-1}K^{-1}$ for natural h-BN, corresponding to an isotopic enhancement of close to 60%. Both measured thermal conductivities either match or exceed previously reported values for bulk crystals, while the isotopic enhancement factor is approximately 35% higher for the isotopically enriched thin crystal compared to the equivalent bulk materials. The work presented here demonstrates isotopic engineering as a viable route to increased thermal conductivity in atomically thin h-BN, making it an outstanding platform material for thermal management in next-generation device applications.

KEYWORDS Hexagonal boron nitride, isotope engineering, thermal conductivity, Raman, two-dimensional materials, interfacial thermal resistance, thermal management

Introduction

Hexagonal boron nitride (h-BN) belongs to a family of layered materials, formed via the strong in-plane covalent bonding of boron (B) and nitrogen (N) atoms with weak van der Waals interactions between the layers. Atomically thin h-BN nanosheets, with a thickness of one to a few

layers, are the two-dimensional (2D) crystalline form of h-BN. Due to a variety of distinguished properties, such as no dangling bonds, an atomically smooth surface, high thermal and chemical stability, high electrical resistivity, and a wide bandgap (~6 eV),[1–3] h-BN nanosheets have been extensively used as a building block for the construction of 2D heterostructures. Such structures represent a new platform for the design of next-generation devices where the desired properties can be tailored for specific applications.[1,4] For instance, graphene devices supported on exfoliated few-layer h-BN show an electron mobility, an order of magnitude higher than those supported on the conventional silicon dioxide (SiO_2) dielectric.[5] Transition metal dichalcogenide (TMDC) devices integrating atomically thin h-BN as a tunneling layer greatly reduces the Schottky barrier, resulting in an improved mobility and output current.[6]

Due to the strong covalent bonding of light B and N atoms, h-BN nanosheets are predicted to have a high in-plane thermal conductivity (k_r) (~500 $Wm^{-1}K^{-1}$ for few-layer h-BN, increasing to ~810 $Wm^{-1}K^{-1}$ for a monolayer)[7], two to three orders of magnitude higher than the SiO_2, glass or polymeric substrates used in current 2D devices. If such a high k_r is achievable in practice, h-BN nanosheets will be a transformative thermal management material for next-generation devices.[1,8] However, only a handful of studies have focused on measuring the thermal conductivity of few layer h-BN, and most of the experimental results to date are far below the predicted value. Jo *et al.*[9] reported a k_r of ~250 $Wm^{-1}K^{-1}$ and ~360 $Wm^{-1}K^{-1}$ for 5-layer and 11-layer h-BN, measured by built-in resistance thermometers on which the h-BN nanosheets were pre-patterned with the aid of poly(methyl methacrylate) (PMMA). An even lower value (~240 $Wm^{-1}K^{-1}$) was reported for CVD grown 9-layer h-BN,[10] measured by an optothermal Raman method where a PMMA-mediated wet-transfer process was also used. These results are below even the value recently measured for bulk

h-BN, 408 $Wm^{-1}K^{-1}$.[11] It is possible that in the aforementioned h-BN nanosheet studies,[9,10] the organic residue (i.e. PMMA) introduced in the wet-transfer processes may hinder the heat conduction in few-layer h-BN and suppress the measured thermal conductivity. However, it is still not clear whether few-layer (5-11 layer) h-BN could have an intrinsic thermal conductivity as high as, or higher than that of bulk crystal.

Some studies have shown that k_r can be enhanced with a thinner and cleaner h-BN nanosheet. For instance, clean bilayer h-BN, fabricated with a PMMA-free dry-transfer process, was measured with a k_r of ~480 $Wm^{-1}K^{-1}$ using the resistance thermometer method.[12] More recently, 3-layer, bilayer and monolayer h-BN, obtained via direct exfoliation onto the target substrate, were reported with k_r ~600 $Wm^{-1}K^{-1}$, ~650 $Wm^{-1}K^{-1}$ and ~750 $Wm^{-1}K^{-1}$, respectively, using the optothermal Raman method.[13] However, the nanosheet fabrication methods used in those studies are challenging, with a very low sample yield[12] or poor compatibility[13] with the general fabrication process of 2D heterostructures.[1,4–6] Such transfer techniques are therefore currently suitable solely for the experimental study of thermal conductivity rather than for wider applications.

Therefore, driving few-layer h-BN thermal conductivity to higher values remains a challenge of great interest for enabling enhanced thermal management in the 2D electronic devices. Here, we report a promising route to enhancing the thermal conductivity of h-BN nanosheets based on boron isotopic enrichment. Naturally occurring boron (B) contains two stable B isotopes (19.9% ^{10}B and 80.1% ^{11}B). Materials with just one boron isotope have a higher thermal conductivity due to the elimination of phonon scattering from isotopic disorder, the random distribution of boron isotopes.

Enhanced thermal conductivity has been experimentally observed in the B isotope purified cubic boron phosphide (c-BP),[14] cubic BN[15] and h-BN bulk materials.[11]

Previous calculations have suggested that the isotope enrichment effect on thermal conductivity could be even larger in low-dimensional BN nanosheets than in the bulk.[7] However, recently the opposite effect was observed experimentally in 1-3L monoisotopic ^{10}B and ^{11}B h-BN.[16] The enhancement factor was reported as only 28% for 1L monoisotopic ^{10}B h-BN compared with 1L natural h-BN, somewhat lower than the enhancement factor measured in the equivalent bulk crystals (43%).[11] This factor was also shown to increase with increasing layer number, and an isotopic enhancement as high as 38% was recorded for 3L ^{10}B h-BN over the equivalent natural h-BN sample. Further study of the enhancement effect in few-layer h-BN of thickness >3L would be particularly advantageous for a few reasons. Firstly, for additional insight into the interplay between thickness and isotopic effects in this material, and secondly, from a technological perspective. Few-nm thick h-BN has been demonstrated to be a more suitable and reliable choice for dielectric or passivation layers in real devices[4] compared with the ultra-thin (1-3L) material. Additionally, difficulties with low sample yield of ultra-thin materials and the extreme sensitivity of their thermal properties to external factors such as sample residues suggest that practically, enhancing the thermal conductivity of few-layer h-BN through isotopic engineering may have more significant implications for real-world thermal management applications.

In this work, two 11-layer h-BN nanosheets were exfoliated from monoisotopic ^{10}B (99% ^{10}B) and natural (22% ^{10}B) h-BN single crystals. Nanosheets were then suspended on a holey support grid by a thin-film transfer process specially developed to produce clean and high-quality samples for thermal conductivity measurements. A finite element analysis (FEA) approach was used to

extract thermal conductivity, with a thorough consideration of the effects of interfacial thermal resistance (ITR) and thermal expansion coefficient (TEC) mismatch induced strain on the measurement. At room temperature, an in-plane thermal conductivity (k_r) as high as (630 +90/-65) $Wm^{-1}K^{-1}$ was measured for the monoisotopic ^{10}B h-BN nanosheet, 57.5% larger than the nanosheet with natural B isotope concentration. The measured k_r of both monoisotopic and natural nanosheets here are higher than all previously reported values of 5- to 11-layer naturally occurring h-BN. Our results illustrate the potential to increase the thermal conductivity with isotope enrichment and thin-film fabrication techniques. These techniques could be directly applied to the thermal management of next-generation devices.

Results and Discussion

Few-layer h-BN Transfer Technique

Few-layer nanosheets were exfoliated from 99% ^{10} B and 22% ^{10}B h-BN single crystals using Scotch tape onto a silicon (Si) substrate covered with ~290 nm-thick thermal oxide (SiO_2). The isotope ratios of the bulk crystals were previously determined when these materials were studied in some of the authors' earlier work.[11] We identified appropriate nanosheets by measuring their thickness with atomic force microscopy (AFM). For the thermal conductivity measurements, it was necessary to transfer and suspend the identified h-BN nanosheets over a hole on a membrane. As shown in Figure 1(a)-1(f), we developed a transfer technique that is a hybrid of the methods described in Refs. [9] and [17], to reduce contamination of the nano-sheets which hindered previous h-BN results published in the literature. A piece of polydimethylsiloxane (PDMS, Sylgard 184 Elastomer kit, Sigma-Aldrich) was placed on top of the identified h-BN on SiO_2/Si

(Figure 1(a)), and the stack was heated at 120 ºC to improve the adhesion between the PDMS and h-BN. After the stack was placed in a 1% hydrofluoric acid (HF) solution for about 10 mins (Figure 1(b)), the interface oxide was etched away so that the PDMS layer along with the h-BN samples was detached from the Si substrate (Figure 1(c)). The floating PDMS/h-BN was picked up with tweezers and dried with nitrogen, and then mounted on a clean glass microscope slide. From this point onwards, we continued with the technique as described in Ref. [17]: the h-BN was dry transferred deterministically using the viscoelastic properties of PDMS on top of the target substrate (Figure 1(d)-(f)). The target substrate was a 50 nm Au-coated holey silicon nitride (Si_3N_4) support membrane with 5 μm diameter holes. Finally, the sample was rinsed with deionized water and annealed at 120 °C to increase the adhesion between the few-layer h-BN and the support membrane. This hybrid transfer technique combines the benefit of easily identifying appropriate nanosheets by using the SiO_2/Si substrate for exfoliation[9] with the advantages from the dry-transfer method,[17] allowing sheets of pre-determined thickness to be transferred quickly and cleanly with a high yield, while enabling easy and accurate positioning of the flake to the target location on the substrate. A detailed assessment of the cleanliness of our transferred samples, and how they compare to previously measured h-BN nanosheets in the literature is included in Section 2 of the Supporting Information.

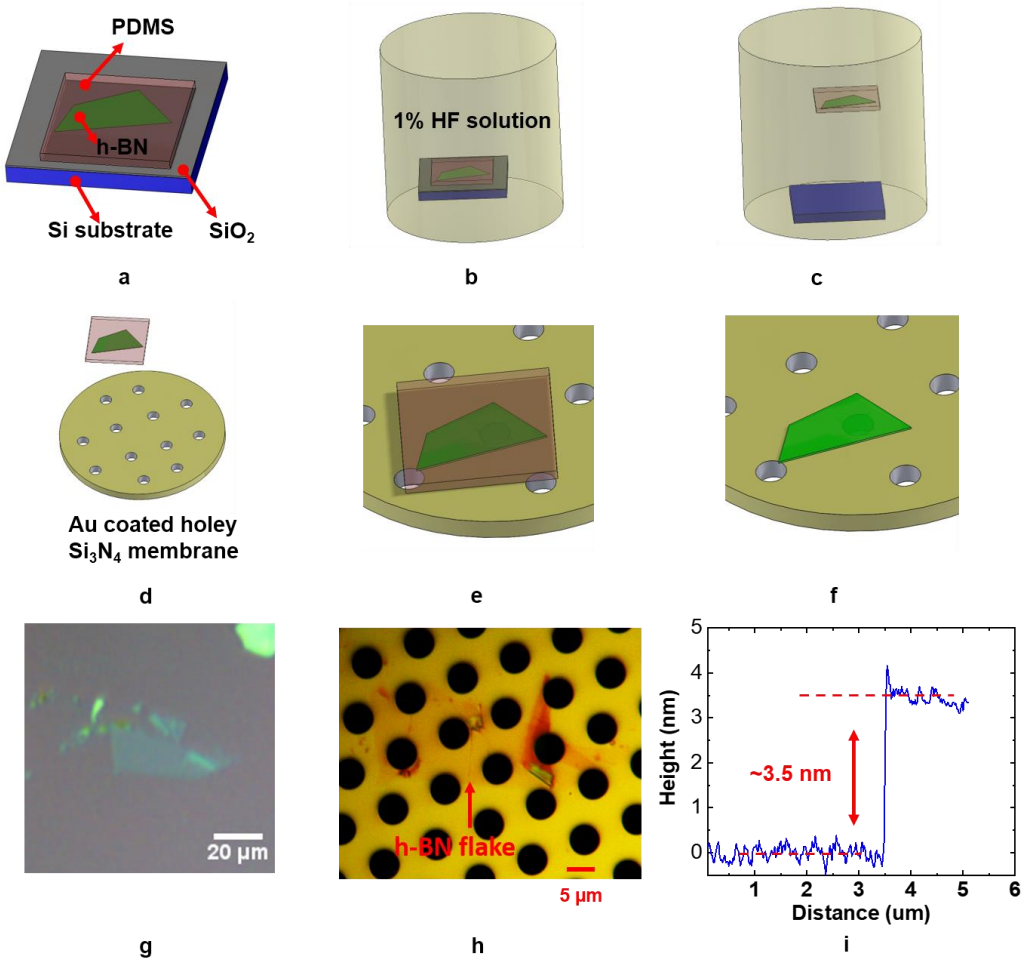

Figure 1. The h-BN transfer process. **(a)** Polydimethylsiloxane (PDMS) was placed on top of the h-BN exfoliated on a SiO_2/Si substrate; **(b)** the PDMS/h-BN/SiO_2/Si stack was placed in a 1% hydrofluoric acid (HF) solution; **(c)** after ~10mins, the SiO_2 was etched away so that the PDMS layer with the h-BN was detached from the substrate; **(d)** h-BN was aligned on top of the target substrate (Au-coated holey Si_3N_4 support membrane); **(e)** PDMS with h-BN was pressed against the substrate; **(f)** PDMS was peeled off and the nanosheet was left suspended over a hole of the Si_3N_4 membrane. Processes **(d)** to **(f)** are from the dry-transfer technique as detailed in Ref. [17]. **(g)** Photograph of the monoisotopic ^{10}B h-BN nanosheet supported on SiO_2/Si before transfer and **(h)** after transfer to an Au-coated Si_3N_4 holey support grid. **(i)** AFM height traces across the edge of the monoisotopic ^{10}B h-BN nanosheet on the SiO_2/Si substrate.

Bulk h-BN single crystals were produced as described by Liu *et al.*[18], using a method that can be exploited to fabricate h-BN with any B isotope concentration. Investigated here are crystals previously studied as bulk materials in Ref. [11] with B isotope compositions of 99% ^{10}B and 22% ^{10}B. The h-BN nanosheets exfoliated from these samples are referred to as 'monoisotopic' and 'natural' h-BN respectively throughout the remainder of this paper. Figure 1(g) shows a transferred few-layer monoisotopic ^{10}B h-BN flake suspended over the holes of the support membrane. Layer thicknesses were determined as ~3.5 nm and ~3.7 nm for the monoisotopic ^{10}B and natural h-BN nanosheets, measured with AFM (results are shown in Figure 1(h) and Figure S1, respectively). As the thickness of an h-BN monolayer is ~0.33 nm,[9] the number of atomic layers in both the monoisotopic ^{10}B and natural nanosheets was estimated to be 11.

Thermal Conductivity Measurements

A modified optothermal Raman method[19,20] combined with finite element thermal analysis was used to measure the in-plane thermal conductivity (k_r) of monoisotopic and natural h-BN flakes. Figure 2a shows the typical room-temperature peak positions of the h-BN E_{2g} mode, centered at 1393cm^{-1} and 1367cm^{-1} for monoisotopic h-^{10}BN and natural h-BN respectively. These are consistent with previously reported values for materials with the same isotopic composition.[11,21,22] A significantly narrowed Raman linewidth for the monoisotopic sample (4.6 cm^{-1}) relative to the natural sample (8.8 cm^{-1}) was observed as a result of the reduced isotopic disorder in this crystal.[22,23] The first-order Raman temperature coefficients (χ_{E2g}) for each sample were extracted as described in the Methods section and results are shown in Figure 2b. We determined the strain-

corrected χ_{E2g} to be -0.0197 ± 0.0007 cm^{-1}/K and -0.0170 ± 0.0007 cm^{-1}/K for the natural and monoisotopic flakes respectively. Both coefficients are consistent with previously reported values for samples in the literature.[13,21,24,25] We used these corrected χ_{E2g} to convert the Raman shifts to measured temperature rise as a function of absorbed laser power ($\theta_m(Q)$), with the results shown in Figure S12 The thermal conductivities were then extracted from these measurements by finite element analysis in ANSYS Academic Research Mechanical, release 19.1 (see details in Supporting Information, Figure S13).

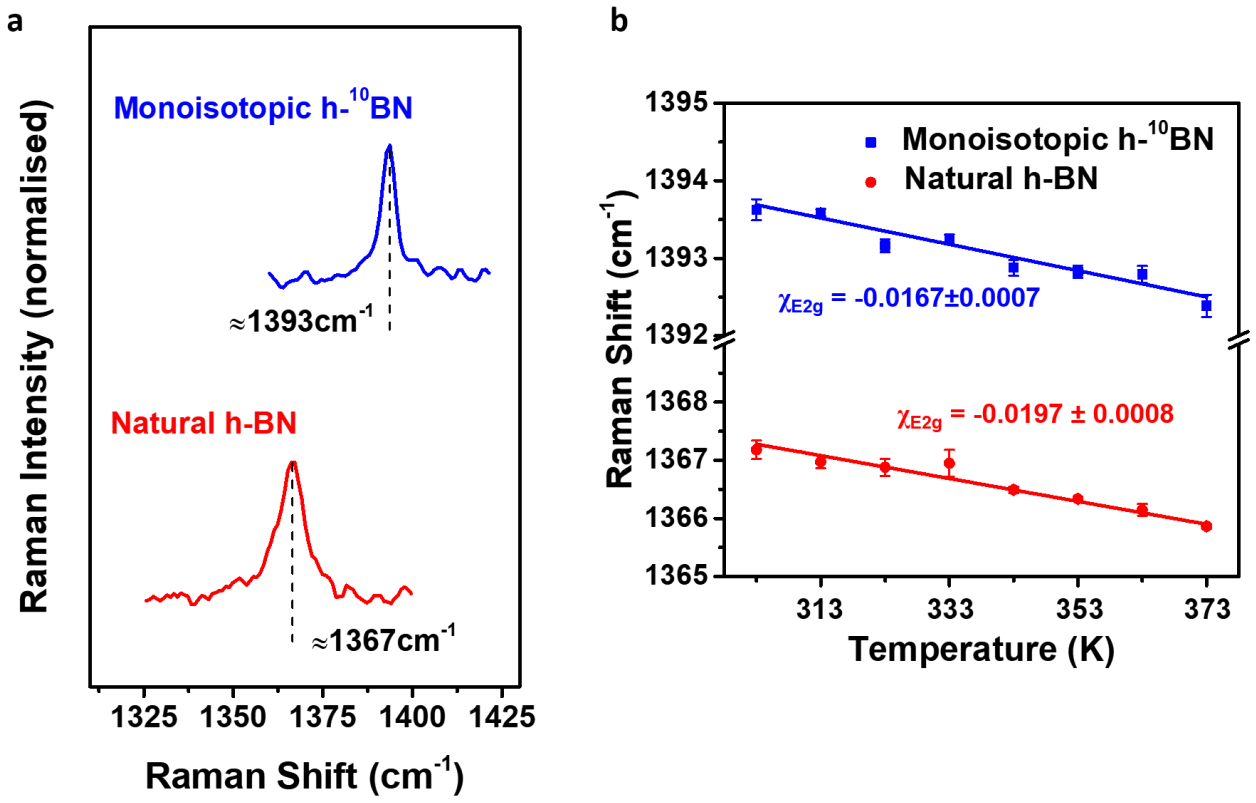

Figure 2. Raman peak position and temperature coefficient (χ_{E2g}) extraction for monoisotopic h-^{10}BN and natural h-BN. a) Typical room temperature Raman spectra of both

samples. b) Raman shift as a function of sample temperature in suspended flakes. Peak shifts have been corrected from strain effects as described in Equation S1. A linear fit to the data has been performed to extract first-order Raman temperature coefficients (χ_{E2g}).

Figure 3a shows the in-plane thermal conductivity (k_r) results for the two 5-μm-diameter suspended h-BN nanosheets obtained from fitting the experimental data to results of a finite element thermal simulation using ANSYS. Also shown are reported k_r calculation results for monolayer and few-layer h-BN based on an exact numerical solution of the Boltzmann transport equation (BTE) incorporating three-phonon, phonon–isotope and boundary scattering processes.[7] At 303K, we measured the k_r of monoisotopic and natural samples to be (630 +90/-65) $Wm^{-1}K^{-1}$ and (405 +87/-65) $Wm^{-1}K^{-1}$, respectively. There is good agreement with the calculation results for 5-layer h-BN close to room temperature. Note that there are a few small discrepancies between the model parameters[7] and the experiment performed here. First, the size (5 μm) of our suspended samples is less than the grain size (10 μm) for the boundary scattering calculation in model. However, this is unlikely to have a significant effect on the interpretation of our results since the size effect on k_r becomes negligible when it is larger than the dominant phonon mean free path (<1 μm).[26] Second, due to the excessive computational demand caused by increasing the number of layers, few-layer samples with a layer number greater than 5, such as those measured here, were not considered in the theoretical calculation.[7] Despite this, note that in Ref [7], the calculated k_r converges to the 5-layer value as the number of layers increases. As a result, we use the calculated value from 5-layer h-BN in Ref. [7] to make an approximate comparison to the k_r for our few-layer h-BN. Finally, the calculated values for monoisotopic h-BN shown are for material with 100% ^{11}B

isotopic composition, rather than ^{10}B as discussed in this work. However, at room temperature, it has been previously reported that the difference in thermal conductivity between monoisotopic h-BN comprised of ^{10}B and ^{11}B isotopes is negligible,[11] so we consider these calculations a reasonable approximation to the material under investigation here. Since the first-principles calculations consider defect-free h-BN with an effective boundary length exceeding the measured sample size, the good agreement with our experimental results suggests there are no significant defects in these samples, neither from within the material itself nor resulting from the transfer process.

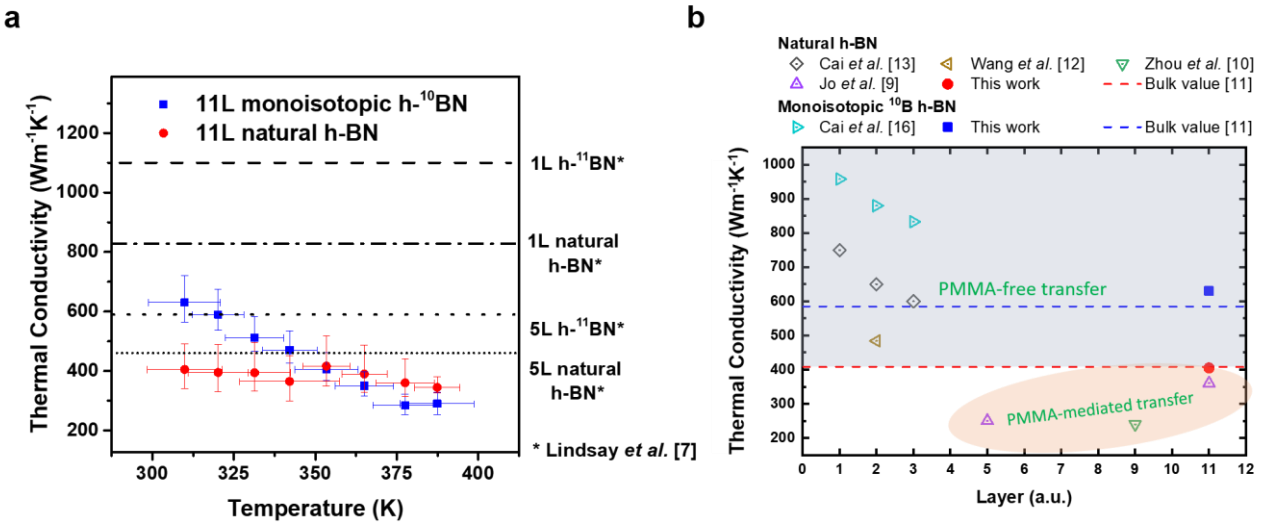

Figure 3. Measured thermal conductivity of 11-layer monoisotopic and natural h-BN. a) Extracted thermal conductivities alongside first-principles calculations for single layer and 5-layer natural h-BN and monoisotopic h-^{11}BN taken from Lindsay *et al.*[7] b) Comparison of room temperature thermal conductivities measured in this work and in the literature. Bulk values are indicated by the dashed lines and approaches using PMMA-mediated and PMMA-free transfer techniques are highlighted.

Figure 3b compares the measurements with literature reported results at room temperature. Note that k_r of the monoisotopic nanosheet is slightly larger than the value previously reported for the raw bulk crystals.[11] Recently, it has been demonstrated experimentally that exfoliating natural h-BN to monolayer thickness achieves superior thermal conductivity,[13] primarily due to a symmetry-based selection rule for phonon scattering in 2D crystals.[7] However, the fabrication processes required to achieve monolayer or bilayer h-BN are particularly challenging, with very low sample yields.[12] Strikingly, our k_r result for isotopically engineered h-BN is comparable to the highest values for extremely thin (1-2 layer) h-BN,[12,13] demonstrating the potential to achieve superior thermal conductivity even in multilayer h-BN. Previous calculations[7] have suggested k_r can be driven to even higher values, >1100 $Wm^{-1}K^{-1}$, with an even larger enhancement factor if monoisotopic h-BN can be reduced to monolayer thickness. However, recently Cai *et al.*[16] (Fig. 3b) reported an enhancement of only 28% for 1L monoisotopic ^{10}B h-BN, significantly lower than both the bulk value (43%)[11] and our 11L value (58%). Cai *et al.*[16] also observed an increase in the isotopic enhancement with increasing layer number, contrary to earlier predictions.[7] While further work is likely required to fully clarify the interplay between thickness and isotopic effects in h-BN, it seems that the benefit of isotopic engineering in h-BN is greater in our thicker material (11L) compared with ultra-thin monolayer h-BN. We find that k_r for the 11-layer nanosheet with natural B isotope composition is approximately in line with previous reports for bulk natural h-BN[11,26], and larger than all previously reported values for h-BN of similar thickness (5 to 11 layer),[9,10] as shown in Figure 3b.

The data presented in Figure 3b also highlights the large spread in measured h-BN thermal conductivity values between different reports. While this can often be attributed to differences in

sample preparation or measurement technique,[27] variations in measured thermal properties may also arise due to inconsistent treatment within the heat conduction model.[28] Here, we have incorporated additional corrective factors, such as TEC mismatch induced strain and finite thermal boundary conductance (g), into the model. These factors are inconsistently applied in experimental studies of 2D materials; they are incorporated in some cases, but not in others. Previous measurements of h-BN thermal conductivity using an optothermal Raman technique have not included these effects,[10,13] so their impact on the final values is not yet fully understood. A detailed analysis of the impact of these factors, in addition to other potential sources of error in our measurement is included in the Supporting Information (Section 10). The uncertainty in optical absorption was the dominant factor contributing to measurement error. Therefore, y-axis error bars shown in Figure 3a correspond to the thermal conductivity values obtained using the upper and lower bounds for absorption. Error bars on the x-axis were calculated using a standard square root sum propagation method, including the uncertainty in the Raman peak positions and from the thermal calibration. Error due to optical absorption uncertainty was calculated to be approximately 12% for the monoisotopic samples, and up to 20% for natural h-BN (Figure S11a), indicating the importance of developing improved methods for *in situ* optical absorbance in this type of measurement. The effect of neglecting the correction for TEC mismatch induced strain led to an overestimation of thermal conductivity by about 5-6% for both samples (Figure S14b), while ignoring the contribution of interfacial thermal resistance (ITR) at the suspended area edge underestimated the final thermal conductivities by between 20-30% (Figure S14c). Similarly large errors resulting from failure to consider ITR in thermal measurements have previously been reported in graphene and GaN.[28] The magnitude of these corrective factors suggests that they should rarely be neglected without thorough justification.

At room temperature, the k_r enhancement due to isotope purification is 58%, demonstrating a large isotopic effect in few-layer h-BN. This is larger than the enhancement (~43%) recently reported for the bulk crystals at this temperature.[11] The increased enhancement factor measured here could be a result of the decreased thickness of the material. It has been well reported for both graphene and h-BN that the room temperature thermal conductivity is heavily modulated by layer number.[7,13,29,30] This effect is primarily the result of the increased cross-plane phonon coupling and availability of additional phase space for phonon-phonon scattering in multi-layered materials. Since increasing the sample thickness increases phonon-phonon scattering rates, it follows that the importance of this type of scattering dominates in thicker flakes over phonon-isotope scattering. Therefore, the influence of isotopic mixing on the thermal conductivity likely decreases with increasing thickness, up until a critical thickness where bulk thermal properties are recovered. Consistent with this, calculations based on a first-principles Boltzmann transport equation (BTE) solution approach have previously revealed a reduction in the isotope enhancement for multilayer samples,[7] indicating that the relative importance of phonon-isotope scattering is diminished when thickness increases.

Despite this, recent reports have shown the opposite trend, revealing an increase in the enhancement for an increasing number of layers for 1-3L samples.[16] This discrepancy can potentially be explained by the underestimation of the importance of optical phonons to phonon-isotope scattering in earlier calculations.[7] Cai *et al.*[16] argued that isotope mixing primarily increases acoustic-optical scatterings between out-of-plane optical (ZO) and longitudinal or transverse acoustic (LA or TA) phonons, whereas the out-of-plane acoustic (ZA) phonons that otherwise dominate transport at room temperature are disproportionately affected by the presence

of additional atomic layers. As a result, ZA phonons contribute a greater proportion of the overall thermal conductivity in natural h-BN, so the detrimental impact of additional atomic layers is larger. Therefore, the percentage decrease in k_r with increasing layer number is smaller for monoisotopic h-BN than natural, which leads to an increased enhancement factor for thicker crystals. However, our results show an enhancement factor greater than that reported for both 1-3L[16] and bulk h-BN,[7] suggesting that the relationship between h-BN thickness and phonon-isotope scattering may be more complex than initially thought.

Relatively few reports have dealt directly with the thickness dependence of h-BN thermal conductivity, and those that have measured thicker (>5L) few-layer flakes have found that their experimental results display the opposite trend[9,10] to theoretical predictions.[7] However, the results in these early experiments can likely be attributed to the larger impact of surface residues on thinner samples.[9] We note that the transfer method reported here can produce cleaner suspended areas than those used in previous works (see Supporting Information, Section 2),[17] contributing to the much higher intrinsic thermal conductivities achieved. In this case, our results suggest that the thermal conductivity of 11L h-BN is higher than, or at least converges to that of the bulk crystal,[11] following the suggested thickness dependence in Ref. [7]. In conventional materials reducing thickness leads to a decrease in thermal conductivity due to phonon-boundary scattering, limiting utility for thermal management in ultrathin devices. By contrast, the unusual thickness dependence of the thermal conductivity of van der Waals materials presents an opportunity for their application in such cases. Our results further highlight this advantage in layered materials, since we were able to achieve very high thermal conductivities, comparable to, or even exceeding that of the bulk materials in films only 3.5nm thick.

At temperatures above 303K, the influence of isotopic disorder on phonon scattering in h-BN diminishes and the thermal conductivity for both the isotopically pure and natural h-BN converges to approximately 375 $Wm^{-1}K^{-1}$. This can be attributed to the increasing importance of phonon-phonon scattering processes at elevated temperatures in competition with the phonon-isotope scattering.[31] A similar effect was observed by Chen *et al.*[32] in monolayer graphene. An isotopic enhancement of 58% was achieved in graphene at room temperature despite a lower level of isotopic mixing in natural graphene (≈1.1% ^{13}C and 98.9% ^{12}C) than natural h-BN. The enhancement was significant even above 500K, whereas for h-BN the enhancement effect is negligible at temperatures greater than approximately 330K. This discrepancy can be explained by considering the relative strength of the in-plane bonds in graphene and h-BN. The B-N bonds in h-BN are considerably weaker than the C-C bonds in graphene, as reflected in the drastically different Debye temperatures of the two materials (410 K for h-BN[33] and 1911 K for graphene[34]). This results in 'softer', lower velocity phonons in h-BN compared with graphene, leading to a significant reduction in isotope scattering rates due to their strong dependence on frequency.[31] Recently it was reported that isotopic enhancement of thermal conductivity is strong in cubic boron nitride (c-BN) even at temperatures as high as 500K.[15] Again, this discrepancy can most likely be attributed to the higher bond strength in cubic versus hexagonal BN and an increased presence of high frequency phonons for isotopic scattering. Since phonon-isotope scattering is reduced in h-BN compared with graphene and c-BN, it would follow that the temperature at which the enhancement effect ceases to be significant is likely below that of these materials, as we have confirmed here.

The thermal conductivity of natural h-BN appears to be independent of temperature in our measurement range (300 - 400K), despite the expectation that it should decrease due to increased phonon-phonon scattering at high temperatures.[31] By contrast, the k_r for monoisotopic h-BN is reduced significantly as a result of increasing temperature. A larger decrease in monoisotopic thermal conductivity in this temperature range is expected from theoretical predictions,[26] since the increased phonon-phonon scattering at higher temperatures contributes a higher proportion of the overall scattering rate compared with the isotopically disordered sample. The overall expected reduction in thermal conductivity for the natural sample is only around 100 $Wm^{-1}K^{-1}$,[26] so it is likely that we were not able to fully resolve the temperature dependence of natural h-BN in this temperature range.

The results presented here demonstrate that isotopic engineering can increase 11L h-BN in-plane thermal conductivity (k_r) to as high as 630 $Wm^{-1}K^{-1}$. A recent study[8] has experimentally shown that adding thin layer of natural h-BN between a graphene device and a SiO_2/Si or flexible glass substrate can greatly reduce the hot-spot temperature in the device. The enhanced k_r observed here in the monoisotopic h-BN nanosheet provides a route to an even more effective heat-spreading material for graphene devices and other next-generation 2D electronic devices via isotopic engineering. In addition, the thin-film transfer technique presented is capable of fabricating relatively clean samples while retaining compatibility with the general fabrication process of h-BN supported heterostructure electronics.[4] Therefore, the high intrinsic thermal conductivity of h-BN can be maintained in devices using this thin-film approach, which is not currently possible with PMMA-mediated wet-transfer processes.[9,10] Apart from 2D thin-film technology, enhanced h-BN thermal conductivity has the potential to also revolutionize thermal management for traditional 3D and 2.5D integrated circuits (ICs) where the nanosheets can either be stacked

together as a heat spreader substrate[35–37] or be used as thermally conductive particles in the thermal interface and encapsulation composite materials.[38,39] The isotopic enhancement of h-BN thermal conductivity in layers of similar thickness to those studied here may be particularly advantageous due to their increased suitability and reliability as a dielectric substrate and heat spreading layer in devices compared with ultra-thin materials.[4]

Conclusions

We investigated the effect of isotopic disorder on the thermal properties of few-layer h-BN by measuring the thermal conductivities of few-layer natural (22% ^{10}B, 78% ^{11}B) and monoisotopic (99% ^{10}B) h-BN. Using an optimized optothermal Raman method with thorough consideration for the effects of finite interfacial thermal conductance and thermal expansion coefficient mismatch induced strain, we extracted values of (630 +90/-65) $Wm^{-1}K^{-1}$ for monoisotopic h-BN and (405 +87/65) $Wm^{-1}K^{-1}$ for natural h-BN at 303K. The 58% enhancement in thermal conductivity in the monoisotopic h-BN thin film close to room temperature is larger than observed in previous studies of the effect of h-BN isotopic disorder in both bulk[11] and 1-3L[16] crystals. The room temperature thermal conductivities of these materials are close to those reported for bulk crystals, demonstrating the potential for application of few-layer h-BN to the thermal management of devices. At temperatures higher than ~355 K, the thermal conductivities of both monoisotopic and natural h-BN converge to approximately 375 $Wm^{-1}K^{-1}$, as anharmonic scattering processes dominate thermal transport. These results highlight the interplay between h-BN thickness and phonon-isotope scattering and provide important information for consideration of isotopically engineered h-BN in thermal management applications.

Methods

Optothermal Raman Measurements

An optothermal Raman method[19,20] was used to measure the in-plane thermal conductivity (k_r) of monoisotopic and natural h-BN flakes. In this technique, the Raman laser light acts as both a heat source and 'thermometer' for the material. The focused laser spot on the sample surface induces a temperature rise in the suspended area, which is measured by means of Raman thermometry. The measured local temperature rise (θ_m) as a function of the total absorbed laser power (Q), along with a reconstruction of the Gaussian laser beam profile and the thermal boundary conditions between the suspended and supported material, was input into a finite element model to extract k_r of the suspended h-BN.

To obtain θ_m, the first-order Raman temperature coefficient (χ_{E2g}) of the E_{2g} peak of h-BN must first be found from a calibration procedure. The Raman E_{2g} peak shift was recorded in response to laser power at discrete temperature points across the whole temperature range (30 ºC-100 ºC) controlled by a thermal stage (THMSG600, Linkam). Due to the low Raman scattering cross-section of h-BN[40] and to avoid excessively long integration times, we used relatively high incident laser powers for this procedure (1.86 mW, 3 mW, 3.75 mW and 5.92 mW) and then decoupled the contribution to the Raman shift due to laser heating from the shift as a result of the ambient sample temperature after the measurement (Figure S6). Details of the extrapolation procedure to eliminate the effect of laser heating and obtain the Raman frequency shift at 0W incident power can be found in the Supporting Information (Section 4). The Raman temperature coefficients (χ_{E2g}) could then be extracted by linearly fitting the data to $\omega - \omega_0 = \chi_{E2g} T$, where ω-ω_0 is the measured Raman frequency shift at 0W incident power and T is the thermal-stage-controlled temperature. Then, χ_{E2g}

was used to convert the raw Raman shifts to local sample temperature as a function of absorbed laser power, $\theta_m(Q)$. Note that the measured Raman shift in the suspended part is partially impacted by the strain induced via thermal expansion coefficient (TEC) mismatch between the suspended part and the connecting supported material.[41] As a result, all suspended h-BN Raman shifts and χ_{E2g} here were corrected for this effect by following a process outlined in Ref. [41]. This procedure is discussed further in Section 6 of the Supporting Information.

Extracting Thermal Conductivity

The thermal conductivity was extracted from the measured $\theta_m(Q)$ by numerically solving the heat equation using a finite element analysis approach in ANSYS Academic Research Mechanical, release 19.1. This method was chosen because it allows accurate reproduction of the Gaussian laser spot profile and the ability to easily explore the impact of a variety of input parameters on the model, such as variations in h-BN optical absorption, supported h-BN thermal conductivity (k_s) and interfacial thermal conductance (g). The thermal conductivity of the suspended h-BN region was a variable parameter, adjusted to achieve a thermal distribution in the laser spot region that matched our $\theta_m(Q)$ measurements (Figure S12). Details of the model can be found in Section 9 of the Supporting Information and Figure S13

The thermal boundary conditions include the supported material thermal conductivity (k_s) and the interfacial thermal conductance (g) between the supported material and TEM substrate. Using the approach outlined in Ref. [19], k_s and g were obtained using two sets of supported area first-order Raman temperature coefficients data measured with two different laser spot sizes (Figure S11).

All Raman measurements were carried out using a Renishaw InVia Raman spectrometer using a 532nm excitation. Prior to all measurements the system was calibrated using a 520.7cm^{-1} Si reference. Measurements performed on the suspended regions of the samples were taken using a Leica 50× 0.6NA objective. For supported measurements, an additional 50× objective was used (0.5NA, Nikon) for the purpose of extracting k_s and g. The laser power dissipated in the suspended samples was measured by placing a laser power meter (Coherent LaserCheck) underneath the sample during measurement and comparing the transmitted power ($P_{covered}$) with that transmitted through an uncovered Si_3N_4 membrane grid hole (P_{empty}). The % absorbed power (a) could then be obtained as $a = 100 \times \frac{(P_{empty} - P_{covered})}{P_{empty}}$ and was found to be 3.39±0.65% and 3.92±0.51% for natural and monoisotopic h-BN respectively. Errors given represent the standard error on the mean of several trials. The laser spot profile was measured by the knife-edge method (Figure S10).

A flowchart illustrating the full measurement and calculation process for each h-BN sample is shown in Figure S5 Details of individual steps and calculations are given in detail in the Supporting Information.

Acknowledgements

E.M. acknowledges funding and support from the Engineering and Physical Sciences Research Council (EPSRC) Centre for Doctoral Training in Condensed Matter Physics (CDT-CMP), Grant No. EP/L015544/1. Support for h-BN crystal growth was provided by the National Science Foundation, grant CMMI 1538127.

References

(1) Akinwande, D.; Petrone, N.; Hone, J. Two-Dimensional Flexible Nanoelectronics. *Nature Communications*. **2014**, 5, 1–12.

(2) Zhang, K.; Feng, Y.; Wang, F.; Yang, Z.; Wang, J. Two Dimensional Hexagonal Boron Nitride (2D-HBN): Synthesis, Properties and Applications. *J. Mater. Chem. C* **2017**, *5*, 11992–12022.

(3) Izyumskaya, N.; Demchenko, D. O.; Das, S.; Özgür, Ü.; Avrutin, V.; Morkoç, H. Recent Development of Boron Nitride towards Electronic Applications. *Adv. Electron. Mater.* **2017**, *3*, 1600485.

(4) Kim, K. K.; Lee, H. S.; Lee, Y. H. Synthesis of Hexagonal Boron Nitride Heterostructures for 2D van Der Waals Electronics. *Chemical Society Reviews*. **2018**, 47, 6342–6369.

(5) Dean, C. R.; Young, A. F.; Meric, I.; Lee, C.; Wang, L.; Sorgenfrei, S.; Watanabe, K.; Taniguchi, T.; Kim, P.; Shepard, K. L.; Hone, J. Boron Nitride Substrates for High-Quality Graphene Electronics. *Nat. Nanotechnol.* **2010**, *5*, 722–726.

(6) Wang, J.; Yao, Q.; Huang, C.-W.; Zou, X.; Liao, L.; Chen, S.; Fan, Z.; Zhang, K.; Wu, W.; Xiao, X.; Jiang, C.; Wu, W.-W. High Mobility MoS $_2$ Transistor with Low Schottky Barrier Contact by Using Atomic Thick h-BN as a Tunneling Layer. *Adv. Mater.* **2016**, *28*, 8302–8308.

(7) Lindsay, L.; Broido, D. A. Theory of Thermal Transport in Multilayer Hexagonal Boron Nitride and Nanotubes. *Phys. Rev. B - Condens. Matter Mater. Phys.* **2012**, *85*, 035436.

(8) Choi, D.; Poudel, N.; Park, S.; Akinwande, D.; Cronin, S. B.; Watanabe, K.; Taniguchi, T.; Yao, Z.; Shi, L. Large Reduction of Hot Spot Temperature in Graphene Electronic Devices

with Heat-Spreading Hexagonal Boron Nitride. *ACS Appl. Mater. Interfaces* **2018**, *10*, 11101–11107.

(9) Jo, I.; Pettes, M. T.; Kim, J.; Watanabe, K.; Taniguchi, T.; Yao, Z.; Shi, L. Thermal Conductivity and Phonon Transport in Suspended Few-Layer Hexagonal Boron Nitride. *Nano Lett.* **2013**, *13*, 550–554.

(10) Zhou, H.; Zhu, J.; Liu, Z.; Yan, Z.; Fan, X.; Lin, J.; Wang, G.; Yan, Q.; Yu, T.; Ajayan, P. M.; Tour, J. M. High Thermal Conductivity of Suspended Few-Layer Hexagonal Boron Nitride Sheets. *Nano Res.* **2014**, *7*, 1232–1240.

(11) Yuan, C.; Li, J.; Lindsay, L.; Cherns, D.; Pomeroy, J. W.; Liu, S.; Edgar, J. H.; Kuball, M. Modulating the Thermal Conductivity in Hexagonal Boron Nitride via Controlled Boron Isotope Concentration. *Commun. Phys.* **2019**, *2*, 43.

(12) Wang, C.; Guo, J.; Dong, L.; Aiyiti, A.; Xu, X.; Li, B. Superior Thermal Conductivity in Suspended Bilayer Hexagonal Boron Nitride. *Sci. Rep.* **2016**, *6*, 1–6.

(13) Cai, Q.; Scullion, D.; Gan, W.; Falin, A.; Zhang, S.; Watanabe, K.; Taniguchi, T.; Chen, Y.; Santos, E. J. G.; Li, L. H. High Thermal Conductivity of High-Quality Monolayer Boron Nitride and Its Thermal Expansion. *Sci. Adv.* **2019**, *5*, eaav0129.

(14) Zheng, Q.; Li, S.; Li, C.; Lv, Y.; Liu, X.; Huang, P. Y.; Broido, D. A.; Lv, B.; Cahill, D. G. High Thermal Conductivity in Isotopically Enriched Cubic Boron Phosphide. *Adv. Funct. Mater.* **2018**, *28*, 1805116.

(15) Chen, K.; Song, B.; Ravichandran, N. K.; Zheng, Q.; Chen, X.; Lee, H.; Sun, H.; Li, S.; Gamage, G. A. G. U.; Tian, F.; Ding, Z; Song, Q.; Rai, A.; Wu, H.; Koirala, P.; Schmidt,

A. J.; Watanabe, K.; Lv, B.; Ren, Z.; Shi, L; Cahill, D. G.; Taniguchi, T.; Broido, D.; Chen, G. Ultrahigh Thermal Conductivity in Isotope-Enriched Cubic Boron Nitride. *Science.* **2020**, *367*, 555–559.

(16) Cai, Q.; Scullion, D.; Gan, W.; Falin, A.; Cizek, P.; Liu, S.; Edgar, J. H.; Liu, R.; Cowie, B. C. C.; Santos, E. J. G.; Li, L. H. Outstanding Thermal Conductivity of Single Atomic Layer Isotope-Modified Boron Nitride. *Phys. Rev. Lett.* **2020**, *125*, 85902.

(17) Castellanos-Gomez, A.; Buscema, M.; Molenaar, R.; Singh, V.; Janssen, L.; van der Zant, H. S. J.; Steele, G. A. Deterministic Transfer of Two-Dimensional Materials by All-Dry Viscoelastic Stamping. *2D Mater.* **2014**, *1*, 011002.

(18) Liu, S.; He, R.; Xue, L.; Li, J.; Liu, B.; Edgar, J. H. Single Crystal Growth of Millimeter-Sized Monoisotopic Hexagonal Boron Nitride. *Chem. Mater.* **2018**, *30*, 6222–6225.

(19) Balandin, A. A.; Ghosh, S.; Bao, W.; Calizo, I.; Teweldebrhan, D.; Miao, F.; Lau, C. N. Superior Thermal Conductivity of Single-Layer Graphene. *Nano Lett.* **2008**, *8*, 902–907.

(20) Cai, W.; Moore, A. L.; Zhu, Y.; Li, X.; Chen, S.; Shi, L.; Ruoff, R. S. Thermal Transport in Suspended and Supported Monolayer Graphene Grown by Chemical Vapor Deposition. *Nano Lett.* **2010**, *10*, 1645–1651.

(21) Cuscó, R.; Artús, L.; Edgar, J. H.; Liu, S.; Cassabois, G.; Gil, B. Isotopic Effects on Phonon Anharmonicity in Layered van Der Waals Crystals: Isotopically Pure Hexagonal Boron Nitride. *Phys. Rev. B* **2018**, *97*, 155435.

(22) Giles, A. J.; Dai, S.; Vurgaftman, I.; Hoffman, T.; Liu, S.; Lindsay, L.; Ellis, C. T.; Assefa, N.; Chatzakis, I.; Reinecke, T. L.; Tischler, J. G.; Fogler, M. M.; Edgar, J. H.; Basov, D.

N.; Caldwell, J. D. Ultralow-Loss Polaritons in Isotopically Pure Boron Nitride. *Nat. Mater.* **2018**, *17*, 134–139.

(23) Cuscó, R.; Artús, L.; Edgar, J. H.; Liu, S.; Cassabois, G.; Gil, B. Isotopic Effects on Phonon Anharmonicity in Layered van Der Waals Crystals: Isotopically Pure Hexagonal Boron Nitride. *Phys. Rev. B* **2018**, 97, 155435.

(24) Stenger, I.; Schu, L.; Boukhicha, M.; Berini, B.; Plaçais, B.; Loiseau, A.; Barjon, J. Low Frequency Raman Spectroscopy of Few-Atomic-Layer Thick HBN Crystals. *2D Mater.* **2017**, *4,* 031003.

(25) Li, X.; Liu, J.; Ding, K.; Zhao, X.; Li, S.; Zhou, W.; Liang, B. Temperature Dependence of Raman-Active In-Plane E2g Phonons in Layered Graphene and h-BN Flakes. *Nanoscale Res. Lett.* **2018**, *13,* 25.

(26) Jiang, P.; Qian, X.; Yang, R.; Lindsay, L. Anisotropic Thermal Transport in Bulk Hexagonal Boron Nitride. *Phys. Rev. Mater.* **2018**, *2*, 064005.

(27) Song, H.; Liu, J.; Liu, B.; Wu, J.; Cheng, H.-M.; Kang, F. Two-Dimensional Materials for Thermal Management Applications. *Joule* **2018**, *2*, 442–463.

(28) Beechem, T.; Yates, L.; Graham, S. Invited Review Article: Error and Uncertainty in Raman Thermal Conductivity Measurements. *Rev. Sci. Instrum.* **2015**, *86*, 041101.

(29) Lindsay, L.; Broido, D. A.; Mingo, N. Flexural Phonons and Thermal Transport in Multilayer Graphene and Graphite. *Phys. Rev. B - Condens. Matter Mater. Phys.* **2011**, *83*, 235428.

(30) Ghosh, S.; Bao, W.; Nika, D. L.; Subrina, S.; Pokatilov, E. P.; Lau, C. N.; Balandin, A. A.

Dimensional Crossover of Thermal Transport in Few-Layer Graphene. *Nat. Mater.* **2010**, *9*, 555–558.

(31) J.M. Ziman. *Electrons and Phonons: The Theory of Transport Phenomena in Solids*. *Oxford University Press, London, UK, 1960*.

(32) Chen, S.; Wu, Q.; Mishra, C.; Kang, J.; Zhang, H.; Cho, K.; Cai, W.; Balandin, a a; Ruoff, R. S. Thermal Conductivity of Isotopically Modified Graphene. *Nat Mater* **2012**, *11*, 203–207.

(33) Khan, A. I.; Navid, I. A.; Noshin, M.; Subrina, S. Thermal Transport Characterization of Hexagonal Boron Nitride Nanoribbons Using Molecular Dynamics Simulation. *AIP Adv.* **2017**, *7*, 105110.

(34) Xie, Y.; Xu, Z.; Xu, S.; Cheng, Z.; Hashemi, N.; Deng, C.; Wang, X. The Defect Level and Ideal Thermal Conductivity of Graphene Uncovered by Residual Thermal Reffusivity at the 0 K Limit. *Nanoscale* **2015**, *7*, 10101–10110.

(35) Fu, L.; Wang, T.; Yu, J.; Dai, W.; Sun, H.; Liu, Z.; Sun, R.; Jiang, N.; Yu, A.; Lin, C.-T. An Ultrathin High-Performance Heat Spreader Fabricated with Hydroxylated Boron Nitride Nanosheets. *2D Mater.* **2017**, *4*, 025047.

(36) Bao, J.; Edwards, M.; Huang, S.; Zhang, Y.; Fu, Y.; Lu, X.; Yuan, Z.; Jeppson, K.; Liu, J. Two-Dimensional Hexagonal Boron Nitride as Lateral Heat Spreader in Electrically Insulating Packaging. *J. Phys. D. Appl. Phys.* **2016**, *49*, 265501.

(37) Choi, I.; Lee, K.; Lee, C. R.; Lee, J. S.; Kim, S. M.; Jeong, K. U.; Kim, J. S. Application of Hexagonal Boron Nitride to a Heat-Transfer Medium of an InGaN/GaN Quantum-Well

Green LED. *ACS Appl. Mater. Interfaces* **2019**, *11*, 18876–18884.

(38) Yu, C.; Zhang, J.; Li, Z.; Tian, W.; Wang, L.; Luo, J.; Li, Q.; Fan, X.; Yao, Y. Enhanced Through-Plane Thermal Conductivity of Boron Nitride/Epoxy Composites. *Compos. Part A Appl. Sci. Manuf.* **2017**, *98*, 25–31.

(39) Yuan, C.; Duan, B.; Li, L.; Xie, B.; Huang, M.; Luo, X. Thermal Conductivity of Polymer-Based Composites with Magnetic Aligned Hexagonal Boron Nitride Platelets. *ACS Appl. Mater. Interfaces* **2015**, *7*, 13000–13006.

(40) Reich, S.; Ferrari, A. C.; Arenal, R.; Loiseau, A.; Bello, I.; Robertson, J. Resonant Raman Scattering in Cubic and Hexagonal Boron Nitride. *Phys. Rev. B - Condens. Matter Mater. Phys.* **2005**, *71,* 205201.

(41) Tian, S.; Yang, Y.; Liu, Z.; Wang, C.; Pan, R.; Gu, C.; Li, J. Temperature-Dependent Raman Investigation on Suspended Graphene: Contribution from Thermal Expansion Coefficient Mismatch between Graphene and Substrate. *Carbon* **2016**, 104, 27–32.

ASSOCIATED CONTENT

Supporting Information

The Supporting Information is available free of charge *via* the Internet at http://pubs.acs.org.

- Optical and AFM characterization of transferred natural h-BN; cleanliness assessment and residue analysis of transferred h-BN flakes; outline of the full measurement procedure and summary of obtained datasets; calibration of the first-order Raman temperature

coefficients; supported h-BN calibration; calculation of thermal expansion coefficient induced strain contribution to Raman shift; determination of laser spot size; calculation of supported h-BN thermal conductivity and interfacial thermal conductance; ANSYS simulation details and calculation of thermal conductivity; uncertainty analysis (PDF)

AUTHOR INFORMATION

Corresponding Author

* Corresponding authors: elisha.mercado@bristol.ac.uk; martin.kuball@bristol.ac.uk

Author Contributions

The manuscript was written through contributions of all authors. ‡These authors contributed equally. All authors have given approval to the final version of the manuscript. E.M., C.Y., Y.Z and M.K. initiated the project and designed the experiments. C.Y. prepared the samples and performed the AFM measurements. E.M performed the thermal measurements and analyzed the data with assistance from Y.Z. J.L synthesized the h-BN bulk crystals under the direction of J.H.E. M.K supervised the project.

For table of contents only